

Porous interpenetrating network hybrids synthesized within high internal phase emulsions

Jenny Normatov, Michael S. Silverstein*

Department of Materials Engineering, Technion – Israel Institute of Technology, Haifa 32000, Israel

Received 1 August 2007; received in revised form 3 September 2007; accepted 5 September 2007

Available online 11 September 2007

Abstract

‘PolyHIPE’ are porous polymers from the polymerization of monomers and crosslinking co-monomers in the continuous phase of high internal phase emulsions (HIPE). Elastomeric polyHIPE have been reinforced through the synthesis of nanocomposites using several different routes including the addition of co-monomers such as vinyltrialkoxysilane, polyhedral oligomeric silsesquioxane (POSS) bearing vinyl groups, or vinyl silsesquioxane (VSQ). This paper describes the synthesis, structure, and properties of hybrid polyHIPE with interpenetrating polymer–inorganic networks synthesized by adding tetraethylorthosilicate (TEOS) to the monomers. The HIPE becomes unstable on addition of 14 mol% TEOS and the resulting polyHIPE contains voids hundreds of micrometers in diameter. On addition of 25 mol% TEOS the large voids become coated with a brittle Si–O shell as the TEOS migrates to the interface between the organic and aqueous phases. In general, the increases in $\tan \delta$ peak temperature, $\tan \delta$ peak breadth, and room temperature modulus with increasing TEOS content are similar to those observed with POSS and VSQ. Unlike the polyHIPE containing vinyltrialkoxysilane, POSS, or VSQ, pyrolysis of these hybrid polyHIPE did not yield porous inorganic monoliths.

© 2007 Elsevier Ltd. All rights reserved.

Keywords: High internal phase emulsion; Hybrid; Interpenetrating networks

1. Introduction

An emulsion in which the internal phase occupies more than 74% of the volume has been termed a high internal phase emulsion (HIPE) [1,2]. ‘PolyHIPE’ are porous polymers that result from the polymerization of monomers and crosslinking co-monomers in a HIPE’s continuous phase. During polymerization, holes develop in the continuous monomer envelope surrounding the discrete droplets owing to changes in surface tension and density [3]. The internal phase can then be removed, leaving a highly porous, open-pore, polymer monolith. Many different monomers and crosslinking co-monomers have been investigated for polyHIPE synthesis and many different polyHIPE-based systems have been developed [1,2,4–15].

PolyHIPE typically have high porosities, high degrees of interconnectivity, and unique micrometer- to nanometer-scale open-pore structures. Such structures are of interest for filtration media, catalysis, chromatography, separation, absorbents, and ion exchange applications [1,2,16–23]. The thermal and mechanical properties for such applications could be enhanced through the synthesis of organic–inorganic hybrids or nanocomposites.

Elastomeric materials are often compounded with reinforcing fillers to improve their mechanical properties. The effectiveness of a filler depends on filler characteristics such as the size and shape of the particles and, more significantly, on the strength of polymer–filler interactions [24]. In systems with strong polymer–filler interactions the extent of reinforcement for a given volume fraction increases as the particle size decreases and the polymer–filler interfacial area increases. Such reinforcing fillers usually have particle diameters in the range of 10–100 nm [25]. The introduction of a molecular-

* Corresponding author.

E-mail address: michaels@tx.technion.ac.il (M.S. Silverstein).

scale reinforcement, a reinforcing molecular network that is intertwined or even interlocked with the polymer should prove even more effective.

Several different approaches have been used to reinforce polyHIPE with inorganic silsesquioxane (SSQ) networks or cages. These include using a vinyltrialkoxysilane co-monomer so that the silsesquioxane network is grafted to the polymer network [26,27]; using a polyhedral oligomeric silsesquioxane (POSS) bearing one vinyl group and seven non-reactive cyclohexyl groups as a co-monomer so that POSS cages are grafted to the polymer network [28]; using a pre-formed vinyl silsesquioxane (VSQ) network as a co-monomer so that the polymer is crosslinked through reaction with the VSQ [29]; and using a pre-formed methyl silsesquioxane (MSQ) network as a non-reactive filler [30]. In general, the $\tan \delta$ peak temperatures, the $\tan \delta$ peak breadths, and the modulus in compression increased with increasing SSQ content [26–30]. It was shown that a reactive SSQ was more effective at enhancing the thermal and mechanical properties than a non-reactive SSQ [30].

This paper describes the synthesis, structure, and properties of hybrid polyHIPE with interpenetrating polymer–inorganic networks using the synthesis approach illustrated schematically in Fig. 1. In Fig. 1, interpenetrating networks are synthesized through the addition of a tetraalkoxysilane (tetraethylorthosilicate, TEOS) to the monomer(s) and crosslinking co-monomer(s) in the organic phase of a water-in-oil (W/O) HIPE. An organic network is formed through the reaction of the monomer(s) and crosslinking co-monomer(s). The alkoxysilane groups undergo hydrolysis to silanol groups followed by condensation with other silanol groups to form Si–O networks and nanoparticles (a sol–gel reaction) [31–36]. As opposed to most of the other hybrid and nanocomposite systems studied previously, in this case there are no covalent bonds formed between the organic and inorganic networks. Instead, the networks should become interlocked by virtue of their simultaneous, but mutually exclusive, synthesis reactions.

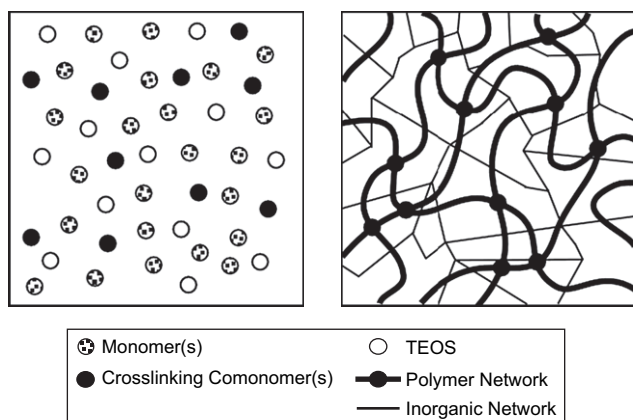


Fig. 1. Schematic illustration of the approach used to synthesize hybrid interpenetrating polymer–inorganic networks.

2. Experimental

2.1. Materials

The monomer used for polyHIPE synthesis was 2-ethylhexyl acrylate (EHA, Aldrich) and the crosslinking co-monomer was divinyl benzene (the term DVB describes the product containing 60% divinyl benzene and 40% ethyl styrene, Riedel-de-Haen). The monomers were washed to remove the inhibitor (once with an aqueous solution of 5 wt% sodium hydroxide (NaOH) and thrice with deionized water). The emulsifier was sorbitan monooleate (SMO, Span 80, Fluka Chemie). The water soluble initiator was potassium persulfate ($K_2S_2O_8$, Riedel-de-Haen). The stabilizer was potassium sulfate (K_2SO_4 , Frutarom, Israel). TEOS (Aldrich) was used as the sol–gel precursor.

2.2. PolyHIPE synthesis and sol–gel reaction

The organic phase of the HIPE contained EHA, DVB, TEOS, and SMO. The EHA/DVB molar ratio was maintained at 74/26. The aqueous phase of the HIPE contained deionized water, initiator, and stabilizer. The mass ratio between the organic phase and the aqueous phase was around 14/86. A typical recipe is listed in Table 1. Various amounts of TEOS (0, 0.5, 1, and 2 g) were added, with the amounts of all the other components held constant. The molar percentages of TEOS in the HIPE, listed in Table 2 and ranging from 0 to 24.6%, are based on the moles of the reactive components (EHA, DVB, and TEOS). The polyHIPE are termed H- x where H stands for ‘hybrid’ and x is the molar percentage of TEOS. The Si contents, listed in Table 2 and ranging from 0 to 2.48%, are based on the amounts of C, O, and Si from the EHA, DVB, and TEOS in the feed. The Si content calculation assumes that one molecule of TEOS becomes SiO_2 . A calculation that assumes that one molecule of TEOS becomes $SiO_{1.5}$ would increase the Si content by, at most, 0.1%.

The polyHIPE synthesis procedure was described in detail elsewhere and is unchanged for the synthesis of these hybrid polyHIPE [6]. The nanocomposite polyHIPE containing POSS, VSQ, or MSQ were synthesized in a similar manner [28–30]. Briefly, the aqueous phase was added slowly to the organic phase with continuous stirring. The resulting HIPE

Table 1
Typical polyHIPE recipe (recipe for H-25)

	Component	Amount (g)	Amount (wt%)
Organic phase	EHA	4	7.50
	DVB	1	1.87
	TEOS	2	3.75
	SMO	1	1.87
	Total	8	15.0
Aqueous phase	H ₂ O	45	84.35
	K ₂ S ₂ O ₈	0.25	0.19
	K ₂ SO ₄	0.1	0.47
	Total	45.35	85.0

Table 2
HIPE compositions and polyHIPE densities

PolyHIPE	TEOS ^a (mol%)	Si ^{a,b} (mol%)	ρ (g/cc)
H-0	0	0	0.13
H-8	7.6	0.66	0.12
H-14	14.0	1.29	0.12
H-25	24.6	2.48	0.13

^a Based on the EHA, DVB, and TEOS in the feed.

^b Based on the C, O, and Si content and assuming that TEOS becomes SiO₂.

was placed in a convection oven at 65 °C for 24 h for polymerization. Following polymerization, the polyHIPE was placed in a vacuum oven at 60 °C for about 48 h for drying. The emulsifier, initiator, and stabilizer were removed by Soxhlet extraction in deionized water for 24 h and in methanol for 24 h. The polyHIPE was then dried in a convection oven at 60 °C for 12 h.

2.3. Characterization

The densities of the polyHIPE were determined using gravimetric analysis. The molecular structures were characterized using photoacoustic Fourier transform infrared spectroscopy (PA-FTIR, Bruker) from 400 to 4000 cm⁻¹ at a resolution of 2 cm⁻¹ and X-ray photoelectron spectroscopy (XPS) (Thermo Sigma Probe, VG Scientific). The porous structure was characterized using high resolution scanning electron microscopy with uncoated specimens and accelerating voltages of 2.5–5 kV (HRSEM, LEO 982, Zeiss). The thermal properties were characterized using dynamic mechanical thermal analysis (DMTA) temperature sweeps at 3 °C/min at a frequency of 1 Hz on 7 × 7 × 7 mm³ cubes in compression (MK III DMTA, Rheometrics). The mechanical properties were characterized using compressive stress–strain measurements on 5 × 5 × 5 mm³ cubes at 25 °C (MK III DMTA, Rheometrics). The measurements were carried out until an equipment-related force limitation was reached. The modulus, E , was calculated from the slope of the stress–strain curve at low strains. Thermogravimetric analysis (TGA) was conducted in air from 25 to 1000 °C at 20 °C/min (2050 TGA, TA Instruments). The differential thermogravimetry (DTG) curves, derivatives of the TGA thermograms, were calculated using the supplied software.

3. Results and discussion

3.1. Molecular structure and porous structure

Si–O networks are generated as TEOS undergoes hydrolysis and condensation. The height of the FTIR band at 1060 cm⁻¹, associated with the Si–O network, increases with increasing TEOS concentration (Fig. 3). There is a small band at 3440 cm⁻¹ in the spectrum of H-0 that is associated with residual emulsifier that is not removed by extraction [5]. This small band appears in all the hybrid polyHIPE. There is no evidence of bands associated with Si–OH at around

3200 and 860 cm⁻¹. The other prominent bands in the FTIR spectra are associated with EHA (C=O at 1730 cm⁻¹, CH₂ at 1461 cm⁻¹, and C–O at 1164 cm⁻¹). The densities of between 0.12 and 0.13 g/cc for the hybrid polyHIPE (Table 2) reflect the volume fractions of the organic phase as calculated from Table 1.

H-0 and H-8 have open-pore morphologies with spherical voids from the evacuated water droplets. The voids are connected by holes in the wall, as seen in Fig. 2(a and b) for H-8. H-8 has voids about 5 μm in diameter and circular holes about 2 μm in diameter. H-0 has a similar structure with larger voids, which are about 15 μm in diameter (not shown). H-14 (Fig. 2c and d) and H-25 (Fig. 2e–g) contain large voids, 200–300 μm in diameter. The thick walls between these large voids have a typical polyHIPE porous structure (Fig. 2c and e), as seen for H-0 and H-8. The number of large voids increases with increasing TEOS content. The HIPE becomes destabilized at the higher TEOS contents resulting in Ostwald ripening, merging of small droplets into larger ones [37]. Ostwald ripening has been observed in other polyHIPE systems and has been related to the reduction in the interfacial tension on addition of relatively hydrophilic moieties to the organic phase [38,39]. In spite of the HIPE destabilization and the associated changes in the porous structure, the HIPE do not collapse and the polyHIPE density remains between 0.12 and 0.13 g/cc.

The inside surfaces of the large voids in H-14 have a nodular structure (Fig. 2d). This nodular structure is similar to the nanoporous structure seen in polyHIPE in which a porogen is added to the co-monomers [26]. The porous structure of H-25 (Fig. 2e) is quite similar to that of H-14 (Fig. 2c) except for some shards of debris on the surface of H-25. As seen for H-14, the areas between the large voids in H-25 have a typical polyHIPE structure. The large voids in H-25, however, seem to be coated with a film that has broken into pieces (Fig. 2f and g). The fracture surface is similar to that observed when a brittle plasma polymerized organosilicon hybrid coating was deposited on a flexible porous organic substrate [40]. The pieces in Fig. 2f fit together to form a shell that coats the inside of the large pores. Beneath the brittle shell in H-25 (Fig. 2g) lies the same nodular structure seen on the surface of the large pores in H-14 (Fig. 2d). These micrographs indicate that, at relatively high TEOS contents, the TEOS migrates to the interface between the organic and aqueous phases. The TEOS at the interface undergoes hydrolysis and condensation, forming a brittle Si–O shell around the water droplets. The shards in Fig. 2e are pieces of that brittle shell.

3.2. Mechanical properties and thermal properties

The variations of E' and $\tan \delta$ with temperature for H-0, H-14, and H-25 are seen in Figs. 4 and 5, respectively. The glass transition temperature, T_g , of PEHA is relatively low and E' begins to decrease with temperature from about –60 °C. E' continues to decrease until a rubbery plateau is reached at around 100 °C. From H-0 to H-14, the $\tan \delta$ peak temperature

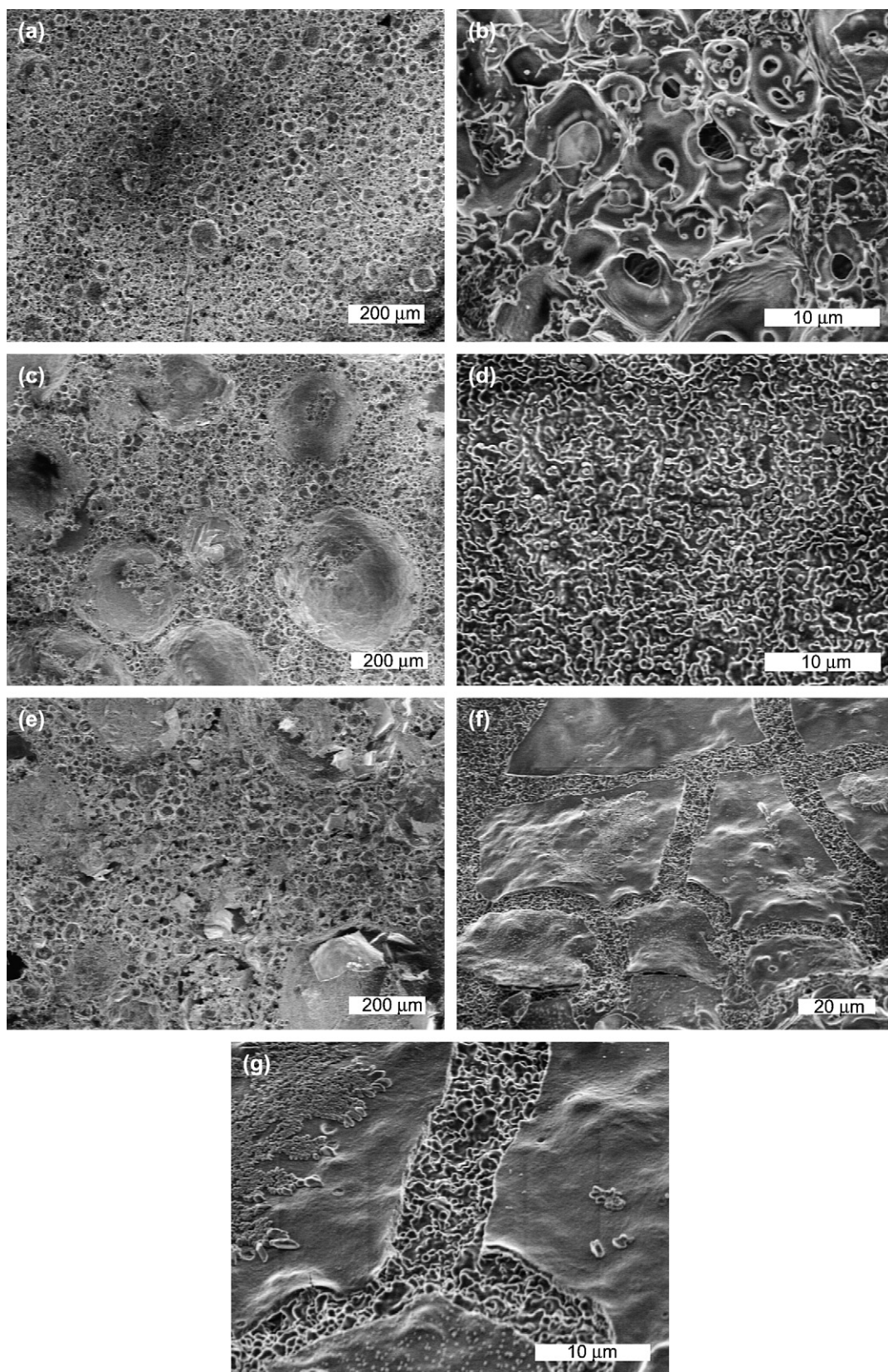


Fig. 2. SEM micrographs of: (a, b) H-8; (c, d) H-14; (e–g) H-25.

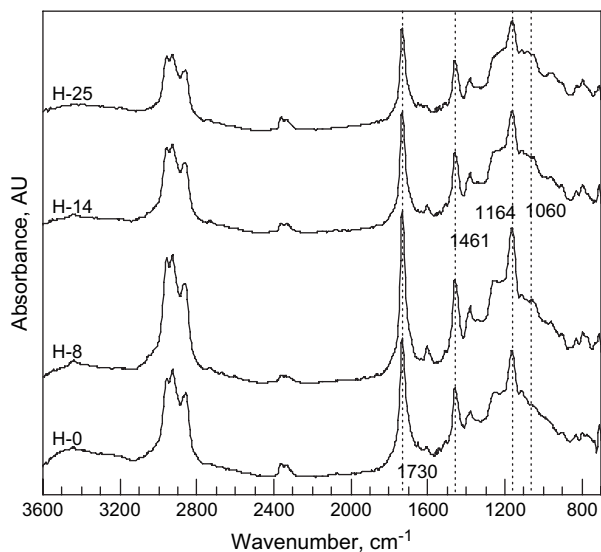
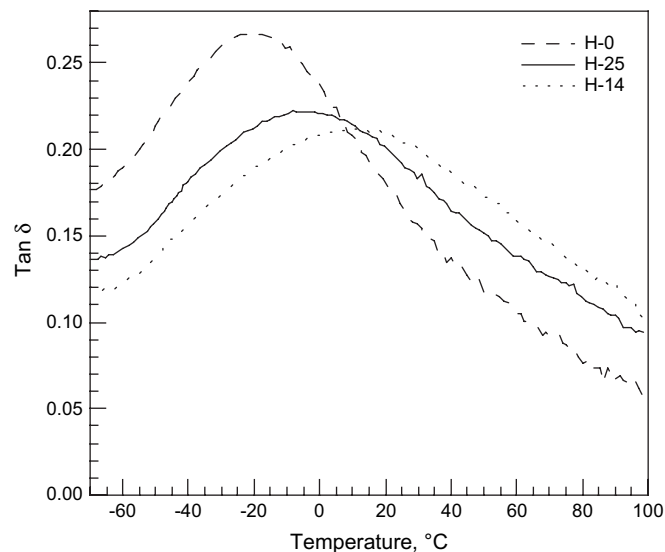


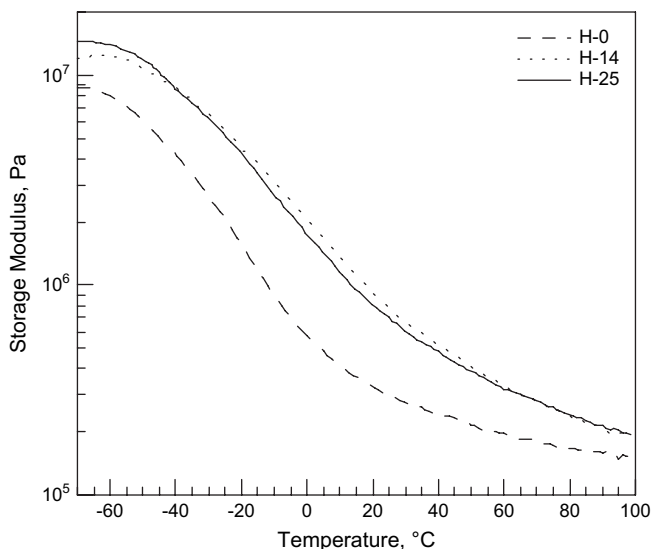
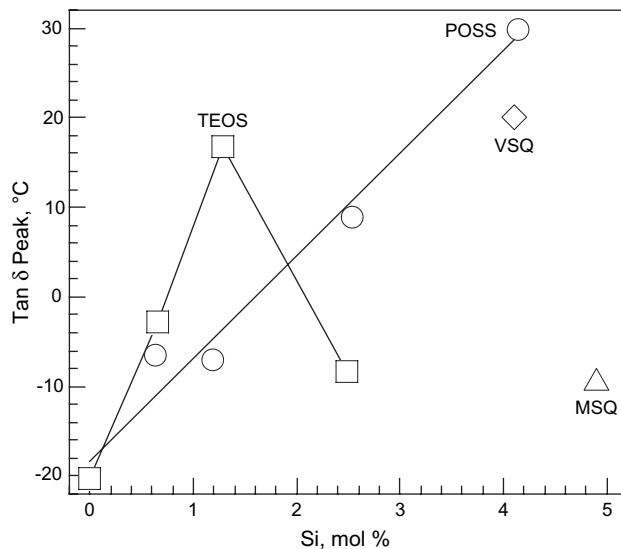
Fig. 3. FTIR spectra for H-0, H-8, H-14, and H-25.

increases by 37 °C. The $\tan \delta$ peak becomes broader and smaller with increasing TEOS content. Such changes have typically been seen for interpenetrating polymer networks containing one rigid network (a polymer below its T_g) and one flexible network (a polymer above its T_g) [41–45]. Here, the Si–O network becomes enmeshed within the polymer network and restricts segmental mobility, raising the $\tan \delta$ peak temperature and broadening the $\tan \delta$ peak. The relatively small increase in the $\tan \delta$ peak temperature for a TEOS content of 25 mol% reflects the segregation of TEOS to the interface between the organic and aqueous phases and the formation of a Si–O coating on the void surfaces, as seen in Fig. 2. The migration of TEOS to the organic/aqueous interface prevents the formation of a more extensive interpenetrating network structure which would have produced a larger

Fig. 5. Variation of $\tan \delta$ with temperature for H-0, H-14, and H-25.

increase in the $\tan \delta$ peak temperature through the limitations on segmental mobility.

The variation of the $\tan \delta$ peak temperature as a function of Si content is seen in Fig. 6. Fig. 6 also includes the variation of the $\tan \delta$ peak temperature with the Si content for the various nanocomposite polyHIPE studied previously [28–30]. All the nanocomposite polyHIPE have EHA/DVB molar ratios of 74/26 and contain POSS, VSQ, or MSQ. The polyHIPE containing MSQ exhibited the smallest increase in the $\tan \delta$ peak temperature, in spite of its relatively high Si content. This increase is relatively small since MSQ does not covalently bond to the polymer network and, therefore, has a smaller effect on segmental mobility. Both VSQ and POSS are covalently bound

Fig. 4. Variation of E' with temperature for H-0, H-14, and H-25.Fig. 6. Variation of the $\tan \delta$ peak temperature with Si content for polyHIPE containing EHA/DVB in a 74/26 molar ratio. (□) TEOS; (○) POSS; (◇) VSQ and (△) MSQ.

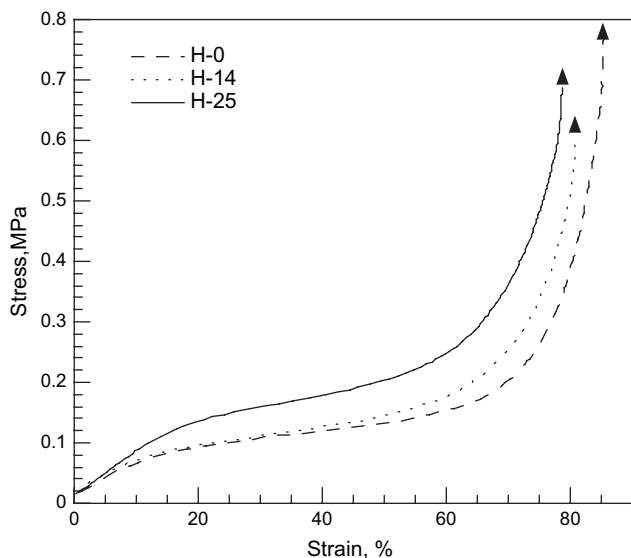


Fig. 7. Compressive stress–strain curves for H-0, H-14, and H-25.

to the polymer network and both produce significant increases in the $\tan \delta$ peak temperature, 40 °C and greater, for Si contents of 4.1 mol%. This increase in the $\tan \delta$ peak temperature reflects the more significant effect that covalent bonding has on the segmental mobility. Interestingly, the initial increase in the $\tan \delta$ peak temperature is largest for the polyHIPE containing TEOS. This relatively large increase indicates that the formation of an interpenetrating network structure is more effective in restricting segmental mobility than grafting POSS cages or crosslinking through a VSQ network. At 25% TEOS, the $\tan \delta$ peak temperature is similar to that of the polyHIPE containing MSQ, reflecting the lack of interaction between the Si–O and the polymer network due to the migration of TEOS to the interface between the organic and aqueous phases.

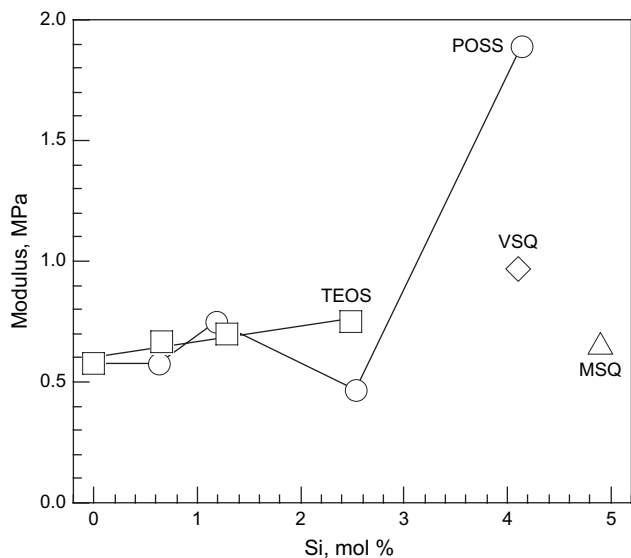


Fig. 8. Variation of the compressive modulus with Si content for polyHIPE containing EHA/DVB in a 74/26 molar ratio. (□) TEOS; (○) POSS; (◇) VSQ and (△) MSQ.

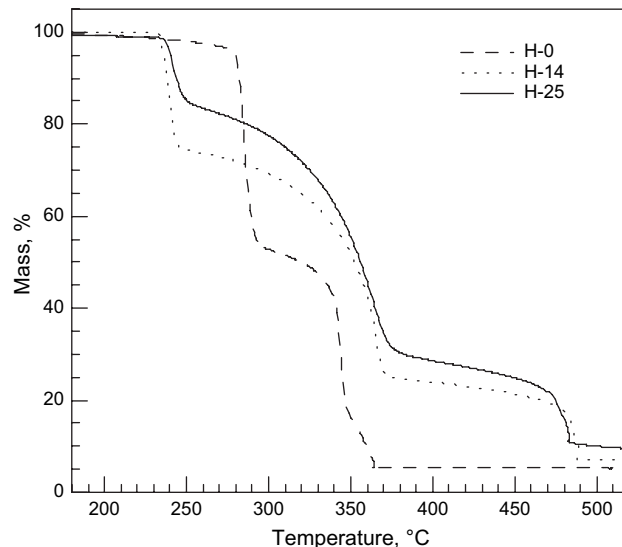


Fig. 9. TGA curves for H-0, H-14, and H-25.

The room temperature compressive stress–strain curves for various hybrid polyHIPE are shown in Fig. 7. All materials exhibit behavior that is typical of polyHIPE: a linear region at low strains, a stress plateau region, and a densification region with a rapid increase in stress. The modulus and the plateau stress increase with increasing TEOS content. These changes in the mechanical properties are consistent with the addition of a relatively stiff filler. The variation of the modulus with Si content in polyHIPE that all have EHA/DVB molar ratios of 74/26 and that contain TEOS, POSS, VSQ, or MSQ is seen in Fig. 8. Interestingly, the increase in modulus as a function of Si content is similar for TEOS, VSQ, MSQ, and all but the highest POSS content. The reinforcement provided by the inorganic component is of similar scales whether the Si–O structure is that of interpenetrating networks, grafted cages, crosslinking filler, or chemically inert filler. The chemically

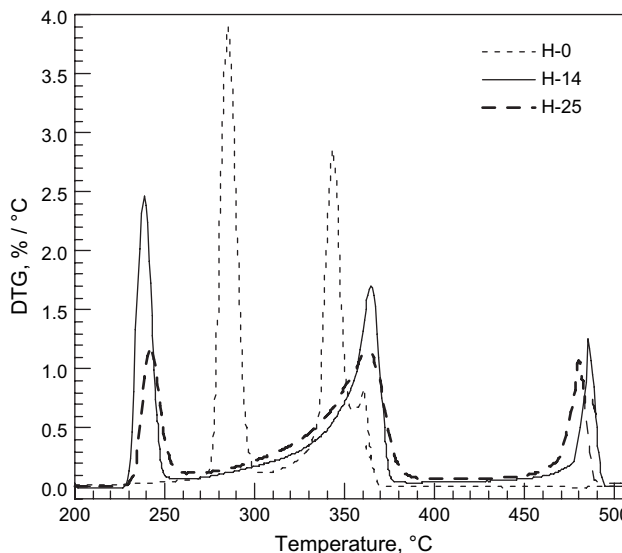


Fig. 10. DTG curves for H-0, H-14, and H-25.

Table 3
Summary of the thermal degradation results

	H-0	H-14	H-25
DTG Peaks (°C)	285 344 (360)	238 365	242 363
T_d (°C)	—	485	480
T_d (°C)	282	237	243
m_R (%)	5.1	7.0	9.1

inert filler, MSQ, yields one of the lowest moduli while the crosslinking filler, VSQ, yields one of the highest moduli. The $\tan \delta$ peak temperature is above room temperature for the polyHIPE with the highest POSS content (Fig. 6). This polyHIPE is, therefore, relatively glassy at room temperature and has a significantly higher modulus.

H-0 exhibits two main degradation stages, the first at 285 °C and the second at 344 °C (TGA and DTG curves in Figs. 9 and 10, respectively). A constant carbonaceous residual mass of 5% is reached at about 370 °C (Table 3). The hybrid polyHIPE exhibits three degradation stages (Figs. 9 and 10). Unexpectedly, the degradation of the hybrid polyHIPE begins at lower temperatures, at around 240 °C. The temperature at which the mass loss reaches 10%, T_d , is around 40 °C lower for the hybrid polyHIPE (Table 3). The temperature of the second degradation stage for the hybrid polyHIPE, 365 °C, is slightly higher than that for H-0. The hybrid polyHIPE exhibits residual mass plateaus of about 25% at around 370 °C. There is an additional degradation stage for the hybrid polyHIPE at around 483 °C. The residual mass increases with the Si content in a linear fashion (Fig. 11) since the origin of the additional residual mass is the Si added to the HIPE. Nanocomposite polyHIPE containing POSS or VSQ exhibit similar increases in residual mass with Si content (Fig. 11).

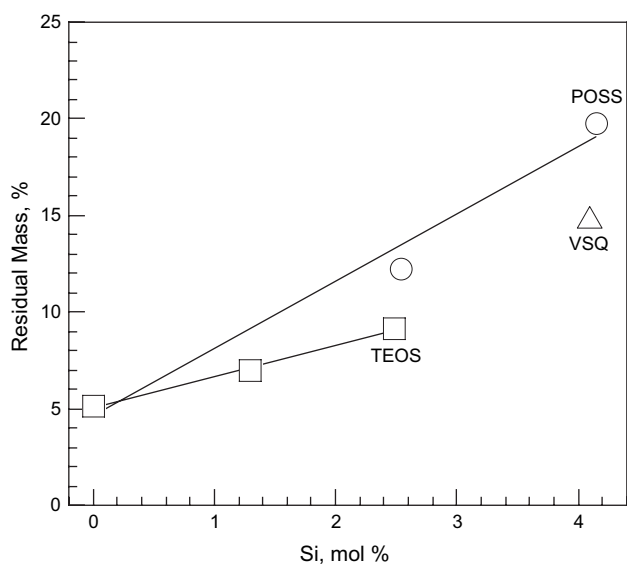


Fig. 11. Variation of the residual mass with Si content for polyHIPE containing EHA/DVB in a 74/26 molar ratio. (□) TEOS; (○) POSS; (◇) VSQ and (△) MSQ.

Ideally, if each Si atom undergoes four hydrolysis–condensation reactions then an SiO_2 network structure is formed. In reality, the reaction reaches various degrees of completion, yielding a looser network. The residual mass following the pyrolysis of H-25 consists of 36.7% Si and 62.2% O (from XPS), yielding the formula $\text{SiO}_{1.7}$. This result is not unusual and has been seen for other hybrid and nanocomposite polyHIPE [26]. Pyrolysis of nanocomposite polyHIPE containing vinyltrialkoxysilane, POSS, or VSQ produced porous inorganic monoliths with porous structures similar to those of the original polyHIPE [26,28,29]. Unlike those polyHIPE, pyrolysis of the polyHIPE containing TEOS did not produce a monolithic structure but, instead, disintegrated into a powder.

4. Conclusions

A hybrid polyHIPE was successfully synthesized through addition of TEOS, a tetraalkoxysilane, to the EHA and DVB in the organic phase. The polyHIPE is unstable at 14 mol% TEOS and Ostwald ripening produces large voids hundreds of micrometers in diameter, as has been seen on addition of hydrophilic moieties to the organic phase in other polyHIPE systems. TEOS is more hydrophilic than the trialkoxysilanes, silsesquioxanes, and POSS studied previously and, unlike most of those materials studied, TEOS does not include a vinyl group that undergoes copolymerization to become covalently linked to the polymer network. The large voids are coated with a brittle Si–O shell at 25 mol% TEOS since TEOS migrates to the interface between the organic and aqueous phases.

The formation of interpenetrating polymer–inorganic networks yields increases in the $\tan \delta$ peak temperature and in the $\tan \delta$ peak breadth. The variation of the $\tan \delta$ peak temperature with the Si content is similar to those seen for nanocomposite polyHIPE containing POSS or VSQ. The Si–O network reinforces the EHA/DVB copolymer, the modulus and the stress plateau increase with increasing TEOS content. Here again, the increase in modulus with Si content is similar to those seen for nanocomposite polyHIPE containing POSS or VSQ. Unlike the polyHIPE containing vinyltrialkoxysilane, POSS, or VSQ, pyrolysis of these hybrid polyHIPE did not yield porous inorganic monoliths.

Acknowledgments

The partial support of the Technion VPR fund is gratefully acknowledged.

References

- [1] Cameron NR, Sherrington DC. *J Mater Chem* 1997;7:2209.
- [2] Cameron NR. *Polymer* 2005;46:1439.
- [3] Cameron NR, Sherrington DC, Albiston L, Gregory DP. *Colloid Polym Sci* 1996;274:592.
- [4] Sergienko AY, Tai H, Narkis M, Silverstein MS. *J Appl Polym Sci* 2004;94:2233.
- [5] Sergienko AY, Tai H, Narkis M, Silverstein MS. *J Appl Polym Sci* 2002;84:2018.
- [6] Tai H, Sergienko A, Silverstein MS. *Polym Eng Sci* 2001;41:1540.

- [7] Desforges A, Backov R, Deleuze H, Mondain-Monval O. *Adv Funct Mater* 2005;15:1689.
- [8] Menner A, Powell R, Bismarck A. *Soft Matter* 2006;4:337.
- [9] Katsoyiannis IA, Zouboulis AI. *Water Res* 2002;36:5141.
- [10] Brown IJ, Clift D, Sotiropoulos S. *Mater Res Bull* 1999;34:1055.
- [11] Sotiropoulos S, Brown IJ, Akay G, Lester E. *Mater Lett* 1998;35:383.
- [12] Livshin S, Silverstein MS. *Macromolecules* 2007;40:6349.
- [13] Haibach K, Menner A, Powell R, Bismarck A. *Polymer* 2006;47:4513.
- [14] Menner A, Haibach K, Powell R, Bismarck A. *Polymer* 2006;47:7628.
- [15] Kulyagin O, Silverstein MS. Porous poly(2-hydroxyethyl methacrylate) hydrogels synthesized within high internal phase emulsions, submitted for publication.
- [16] Krajnc P, Leber N, Brown JF, Cameron NR. *React Funct Polym* 2006;66:81.
- [17] Krajnc P, Stefanec D, Brown JF, Cameron NR. *J Polym Sci Part A Polym Chem* 2005;43:296.
- [18] Krajnc P, Leber N, Stefanec D, Kontrec S, Podgornik A. *J Chromatogr A* 2005;1065:69.
- [19] Akay G, Erhan E, Keskinler B. *Biotechnol Bioeng* 2005;90:180.
- [20] Erhan E, Yer E, Akay G, Keskinler B, Keskinler D. *J Chem Technol Biotechnol* 2004;79:195.
- [21] Moine L, Deleuze H, Maillard B. *Tetrahedron Lett* 2003;44:7813.
- [22] Deleuze H, Maillard B, Mondain-Monval O. *Bioorg Med Chem Lett* 2002;12:1877.
- [23] Zhang H, Hardy GC, Khimyak YZ, Rosseinsky MJ, Cooper AI. *Chem Mater* 2004;16:4245.
- [24] Bokobza L. *Macromol Symp* 2001;169:243.
- [25] Bokobza L. *J Appl Polym Sci* 2004;93:2095.
- [26] Silverstein MS, Tai H, Sergienko A, Lumelsky Y, Pavlovsky S. *Polymer* 2005;46:6682.
- [27] Tai H, Sergienko A, Silverstein MS. *Polymer* 2001;42:4473.
- [28] Normatov J, Silverstein MS. Highly porous elastomer-silsesquioxane nanocomposites synthesized within high internal phase emulsions, submitted for publication.
- [29] Normatov J, Silverstein MS. Silsesquioxane-crosslinked porous nanocomposites synthesized within high internal phase emulsions, *Macromolecules*, in press.
- [30] Normatov J, Silverstein MS. Interconnected silsesquioxane–organic networks in porous nanocomposites synthesized within high internal phase emulsions, submitted for publication.
- [31] Gao Y, Choundhury NR, Dutta N, Matisons J, Reading M, Delmotte L. *Chem Mater* 2001;13:3644.
- [32] Sanchez C, Livage J, Henry M, Babboneu F. *J Non-Cryst Solids* 1988;100:65.
- [33] Chuho Y, Saegusa T. *Adv Polym Sci* 1992;10:11.
- [34] Wen J, Wilkes GL. *Chem Mater* 1996;8:1667.
- [35] Mark JE, Jiang CY, Wilkes GL. *Macromolecules* 1984;17:2613.
- [36] Schubert U, Husing N, Lorens A. *Chem Mater* 1995;7:2010.
- [37] Ostwald W. *Kolloid-Z* 1910;6:103.
- [38] Carnachan RJ, Bokhari M, Przyborski SA, Cameron NR. *Soft Matter* 2006;2:608.
- [39] Lumelski J, Zoldan J, Levenberg S, Silverstein MS. Porous polycaprolactone–polystyrene semi-interpenetrating polymer networks synthesized within high internal phase emulsion polymers, submitted for publication.
- [40] Zuri L, Silverstein MS, Narkis M. *Polym Eng Sci* 1997;37:1188.
- [41] Silverstein MS, Narkis M. *J Appl Polym Sci* 1990;40:1583.
- [42] Silverstein MS, Narkis M. *Polym Eng Sci* 1989;29:824.
- [43] Silverstein MS, Narkis M. *J Appl Polym Sci* 1987;33:2529.
- [44] Thomas DA, Sperling LH. In: Paul DR, Newman S, editors. *Polymer blends*, vol. 2. New York: Academic Press; 1978. p. 20–9.
- [45] Sperling LH. *Interpenetrating polymer networks and related materials*. New York: Plenum Press; 1981. p. 135–55.